Biosensors and Bioelectronics 179 (2021) 113073

Contents lists available at ScienceDirect

Biosensors and Bioelectronics

journal homepage: http://www.elsevier.com/locate/bios

An ultrasensitive CRISPR/Cas12a based electrochemical biosensor for *Listeria monocytogenes* detection

Fan Li [a,b,1], Qinghua Ye [a,1], Moutong Chen [a,1], Baoqing Zhou [a,b], Jumei Zhang [a], Rui Pang [a], Liang Xue [a], Juan Wang [c], Haiyan Zeng [a], Shi Wu [a], Youxiong Zhang [a], Yu Ding [d,**], Qingping Wu [a,*]

[a] Guangdong Provincial Key Laboratory of Microbial Safety and Health, State Key Laboratory of Applied Microbiology Southern China, Guangdong Institute of Microbiology, Guangdong Academy of Sciences, Guangzhou, China
[b] School of Biology and Biological Engineering, South China University of Technology, Guangzhou, China
[c] College of Food Science, South China Agricultural University, Guangzhou, China
[d] Department of Food Science and Technology, Jinan University, Guangzhou, China

ARTICLE INFO

Keywords:
CRISPR biosensor
Electrochemical biosensor
Listeria monocytogenes
Cas12a
Nucleic acid detection
Point-of-care

ABSTRACT

Listeria monocytogenes is an important foodborne pathogen that can cause listeriosis with high patient mortality. Accordingly, it is necessary to develop a *L. monocytogenes* detection platform with high specificity, sensitivity, and exploitability. CRISPR/Cas systems have shown great potential in the development of next-generation biosensors for nucleic acid detection, owing to the trans-cleavage capabilities of the Cas effector proteins. Herein, we introduce the trans-cleavage activity of CRISPR/Cas12a into an electrochemical biosensor (E-CRISPR), combined with recombinase-assisted amplification (RAA), to establish a cost-effective, specific and ultrasensitive method; namely RAA-based E-CRISPR. The concept behind this approach is that the target will induce the number change of the surface signaling probe (containing an electrochemical tag), which leads to a variation in the electron transfer of the electrochemical tag. The introduction of an RAA-based Cas12a system into the E-CRISPR sensor achieves a more prominent signal change between the presence and absence of the target. Under optimized conditions, RAA-based E-CRISPR can detect as low as 0.68 aM of genomic DNA and 26 cfu/mL of *L. monocytogenes* in pure cultures. More importantly, the RAA-based E-CRISPR enables rapid and ultrasensitive detection of *L. monocytogenes* in spiked and natural *Flammulina velutipes* samples. Moreover, no cross-reactivity with other non-target bacteria was observed. This system thus demonstrates to be a simple, high-sensitivity, and high-accuracy platform for *L. monocytogenes* detection.

1. Introduction

Listeria monocytogenes is an opportunistic and dangerous pathogen that can cause listeriosis in humans; it can be particularly serious in pregnant women, children, the elderly, and immunosuppressed individuals (McLauchlin, 1990). *L. monocytogenes* infection causes a greater number of hospitalizations and has a higher mortality rate, with an average post-infection mortality rate of 20%–30% (Lomonaco et al., 2009). Tracking *L. monocytogenes*-related outbreaks showed that it can survive in a variety of foods, and also has the capacity to resist harsh processing conditions (Chen et al., 2018b, 2019b). This adaptation to various food materials and resistance means that *L. monocytogenes* continuously contaminates foods at different stages of food development, from production and processing to packaging and distribution (Chen et al., 2014). Hence, sensitive, inexpensive, and innovative methods are required for the effective detection and identification of *L. monocytogenes* to ensure food safety and protect human health.

The clustered regularly interspaced short palindromic repeats (CRISPR)-associated (Cas) systems are a type of adaptive immune system found in bacteria and archaea that naturally protect against

* Corresponding author. Guangdong Institute of Microbiology, Yard 100#, Xianlie Zhong Lu, Yuexiu District, 510070, Guangzhou, PR China.
** Corresponding author. Department of Food Science & Technology, Institute of Food Safety and Nutrition, Jinan University, Huangpu Ave. 601, Guangzhou, 510632, China.
E-mail addresses: dingyu@jnu.edu.cn (Y. Ding), wuqp203@163.com (Q. Wu).
[1] Fan Li, Qinghua Ye, and Moutong Chen contribute to the manuscript equally.

https://doi.org/10.1016/j.bios.2021.113073
Received 30 November 2020; Received in revised form 28 January 2021; Accepted 2 February 2021
Available online 5 February 2021
0956-5663/© 2021 Elsevier B.V. All rights reserved.

invading nucleic acids (Horvath and Barrangou, 2010). These systems mainly work by targeting and cleaving the invasive DNA sequences. Since the CRISPR/Cas9 system was first applied for gene editing in the mammalian genome, CRISPR/Cas systems have explosively grown in the field of biotechnology and they have become an important tool for transcriptional regulation and genome editing, among other applications (Konermann et al., 2015; Tang and Fu, 2018). More recently, CRISPR/Cas effectors such as Cas13 and Cas12 have been deployed in nucleic acid detection (Chen et al., 2018a; Gootenberg et al., 2017, 2018). Both Cas13 and Cas12 display remarkable potential in developing novel biosensors for nucleic acid detection due to their unique properties of providing signal readouts when target nucleic acids and single-stranded non-targeted nucleic acids (employed as reporters) are cleaved (Dai et al., 2020; Van Dongen et al., 2020; Wang et al., 2020). For example, a Cas13a-based molecular detection platform termed Specific High-sensitivity Enzymatic Reporter unLOCKing (SHERLOCK) has been developed to detect specific strains of Zika and dengue virus, distinguish pathogenic bacteria, genotype human DNA, and identify mutations in cell-free tumor DNA (Gootenberg et al., 2017; Myhrvold et al., 2018). Similarly, by combining Cas12a single-stranded-DNase activation with isothermal amplification, a method called DNA Endonuclease-Targeted CRISPR Trans Reporter (DETECTR) has also been reported for the rapid and specific detection of human papilloma virus in patient samples (Chen et al., 2018a). These systems show great promise by providing sensitivity and single-base specificity. Nevertheless, the readout in these systems mainly rely on fluorescent reporters or lateral-flow strips. Although the lateral-flow detection method was reported to rapidly and accurately readout the signal, it requires complicated systems and tedious sample/reagent processing steps, moreover, the sensitivity was moderately reduced when compared to quantitative-PCR assays (Huang et al., 2020). The fluorescence detection system relied on expensive fluorescence reader equipment, which can cause practical inconvenience and make the system less robust. Hence, simple and ultrasensitive readout methods with a point-of-care capability would enhance the performance of CRISPR-based nucleic acid detection platforms and broaden their applications and functionality.

Electrochemical-based biosensing platforms have been developed due to their fast signal readouts, biosensing platform simplicity, and affordable transduction elements, which provide for a practical and deployable point-of-care system (Dai and Liu, 2019; Dai et al., 2019; Kim et al., 2019; Xu et al., 2020). One of the most common electrochemical biosensing systems for nucleic acid detection and analysis is the electrochemical DNA (E-DNA) biosensor. The E-DNA sensor utilizes the conformational or number change of the surface probe after the introduction of the target, this then induces an electrochemical signal change through the variation in either the contact-mediated electron transfer distance or the number of contact-mediated electrons (Arroyo-Curras et al., 2018; Dai et al., 2019; Dauphin-Ducharme et al., 2019; Xu et al., 2020). Generally, E-DNA sensors using single-stranded DNA (ssDNA) or double-stranded DNA (dsDNA) as interfacial probes possess superior analytical performance, in terms of sensitivity, when compared with the fluorescence transducer.

In this study, we intended to introduce recombinase-assisted amplification (RAA)-based CRISPR/Cas12a into an E-DNA biosensor platform (RAA-based E-CRISPR) for ultrasensitive and specific *L. monocytogenes* detection (Fig. 1). Briefly, a three-electrode electrochemical workstation was applied for the development of the electrochemical biosensor, with gold as the working electrode (diameter, 2.0 mm), platinum as the counter electrode, and Ag/AgCl as the reference electrode. The guide CRISPR RNA (crRNA) was designed to specifically recognize the target DNA based on the target's protospacer adjacent motif (PAM) sequence

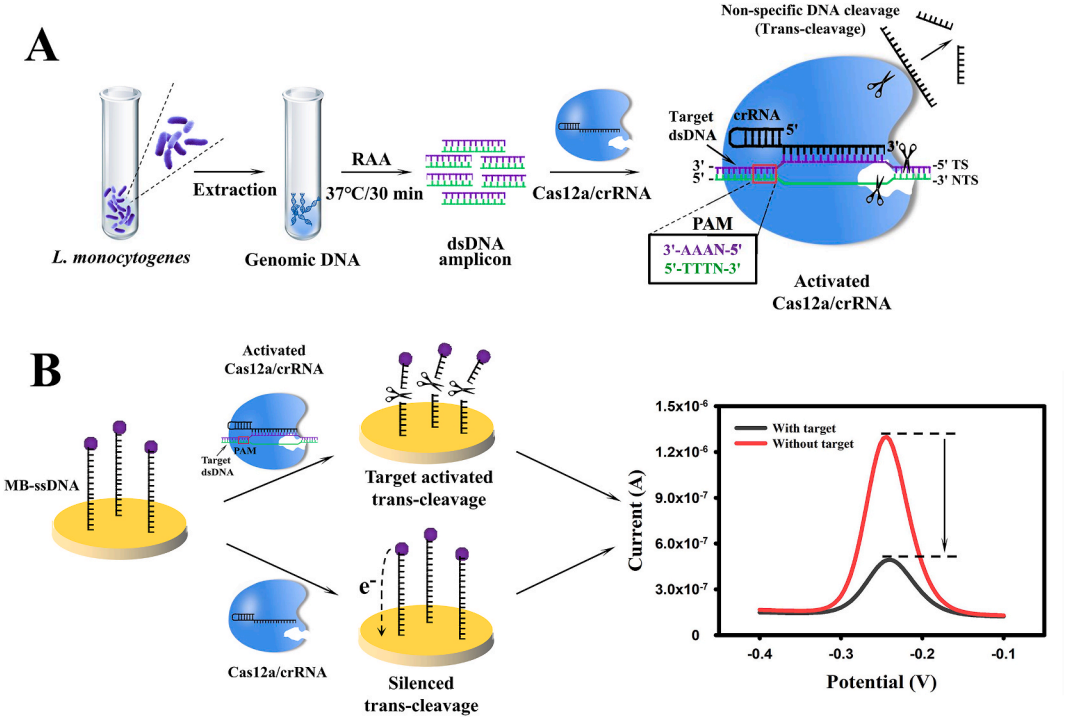


Fig. 1. Principle of the RAA-based E-CRISPR biosensor. (A) Genomic DNA is extracted, RAA-amplified, and then subjected to the Cas12a tran-cleavage reaction. The Cas12a-crRNA duplex binds target dsDNA and generates a 5′-overhang staggered cleavage. The activation of cis-cleavage activity further induces the trans-cleavage activity of the nonspecific ssDNA reporter. (B) Application of E-CRISPR platform to detect RAA products. Nonspecific ssDNA reporters with a methylene blue tag (MB-ssDNA) immobilized on the gold electrode. In the presence of the target, the trans-cleavage activity of Cas12a would be activated, cleaving the MB-ssDNA reporter off the electrode surface, resulting in a low electrochemical current. In the absence of the target, Cas12a/crRNA would not initiate the trans-cleavage activity of the nonspecific MB-ssDNA reporter, resulting in a high electrochemical current. (For interpretation of the references to colour in this figure legend, the reader is referred to the Web version of this article.)

and its complementarity with crRNA. After the Cas protein recognizes the PAM sequence, it unleashes indiscriminate ssDNA trans-cleavage activity, thereby cleaving non-target ssDNA. To achieve the electrochemical transduction of the RAA-based Cas12a detection signal, a nonspecific ssDNA reporter modified with methylene blue (MB) (MB-ssDNA reporter) was assembled on the working electrode through the Au-S covalent bond. In the presence of the target bacteria, the trans-cleavage ability of Cas12a is activated by the RAA-amplified target nucleic acid, cleaving the MB-ssDNA reporter off the electrode surface. At this stage, a differentiable electrochemical signal, before and after the introduction of the target nucleic acid to the sensor, is acquired by squarewave voltammetry (SWV). The design of the MB-ssDNA modified electrode is generally applicable for the Class 2 CRISPR system (i.e., Cas9, Cas12b, Cas13a, and Cas13b), producing a simple and cost-effective active CRISPR transduction strategy. In combination with the RAA, this E-CRISPR biosensor can be used as a novel ultrasensitive and highly-specific biosensing platform for future pathogen detection.

2. Materials and methods

2.1. Materials

Primer sets were synthesized by the Shanghai Generay Biotech Co., Ltd (China). Other oligonucleotides, including the crRNA, ssDNA-FQ reporter, and MB-ssDNA reporter were synthesized by Sangon Biotech (Shanghai) Co., Ltd. (Shanghai, China) (Table S1). EnGen® Lba Cas12a and NEBuffer™ 2.1 were purchased from New England Biolabs Ltd. (New England, USA). RAA basic kit was purchased from Jiangsu Qitian Gene Biotechnology Co., Ltd. (Jiangsu, China). Tris-(2-carboxyethyl) phosphine hydrochloride (TCEP) and 6-mercaptohexanol (MCH) were purchased from Sigma-Aldrich Co., Ltd. (St. Louis, USA). All electrochemical measurements were performed on a CHI 660E electrochemical workstation (Shanghai Chenhua Instrument Co. Ltd., China).

2.2. Bacterial culture and genomic DNA extraction

A total of 15 bacterial strains were used in this study; including 3 *L. monocytogenes* strains (belonging to serotypes 1/2a, 1/2b, and 4b), 5 other *Listeria* strains, and 7 non-*Listeria* strains (Table S2). All the strains were inoculated in brain heart infusion (BHI) medium overnight at 37 °C. Then, 1 mL of each bacterial culture suspension was used for DNA extraction using the DNeasy blood and tissue kit (Qiagen, Shanghai, China) according to the manufacturer's instructions. The purity and concentration of 50 μL of the obtained genomic DNA was measured using the Qubit® 3.0 Fluorometer (Life Invitrogen, USA); it was then stored at −20 °C in preparation for the RAA tests.

2.3. RAA amplification

Primers for the RAA reaction were designed based on the *LMOSLCC2755_0090* gene specific for *L. monocytogenes* using the Oligo 7.0 software (Li et al., 2021). The lengths of the forward and reverse primers were 35 and 34 nucleotides (nt), respectively, and the expected amplicon size was 260 bp (Table S1). The RAA reactions were performed according to the instructions of the RAA basic kit with slight modifications. Briefly, RAA pellets were resuspended in 25 μL of the supplied rehydration buffer. Each reaction contained 10 μL of this RAA rehydration solution, 0.4 μM of forward and reverse primers, 2 μL of target DNA template, 20 mM of magnesium acetate (MgAc), and finally it was made up to 20 μL with sterile water. The mixture was then amplified at 37 °C for 30 min.

2.4. Fabrication of the MB-ssDNA reporter modified gold electrode surface

Before modification, a chemical cleaning procedure was applied to remove any oxides and particles on the surface of the biosensor, thereby reducing the electrode charge transfer resistance. Briefly, the gold electrode was immersed in piranha solution for 5 min, this was followed with the polishing of the gold disk electrode using 0.3 and 0.05 μm alumina in sequence. After polishing it was rinsed thoroughly with distilled water, and then the electrode was immersed in ethanol and distilled water in sequence for 5 min each. Finally, the electrode was electrochemically treated in fresh 0.5 M H_2SO_4 solution until a stable voltammogram was observed. After washing again with distilled water, the electrode was dried with nitrogen gas for further electrochemical applications.

The MB-ssDNA reporter was treated with 10 μM TCEP to reduce the S-S bond in the dark at 37 °C for 2 h. After treatment, the MB-ssDNA reporter was diluted to 1 μM using 10 mM Tris buffer containing 100 mM NaCl, 10 mM $MgCl_2$, and 10 mM EDTA. The diluted MB-ssDNA reporter was directly incorporated onto the gold electrode surface at 37 °C in the dark for 5 h. Then, the MB-ssDNA immobilized electrode was immersed in 10 mM Tris buffer for 5 min. After cleaning, the sensor was immersed in 2 mM MCH, prepared in 10 mM Tris buffer overnight at 4 °C, to passivate the surface and replace any loosely attached MB-ssDNA reporter and form a highly aligned surface. After the MCH treatment, the sensor was immersed and rinsed in 10 mM Tris buffer to remove any non-absorbed residual molecules. The cleaned sensor was then dried with nitrogen gas and prepared for processing with the CRISPR system. For short-term storage, the cleaned sensor can be stored in 10 mM Tris buffer (containing 100 mM NaCl) at 4 °C.

2.5. In vitro digestion of Cas12a-crRNA

For electrochemical analysis of trans-cleaved reporters, the cleavage assay was carried out with slight modifications (Dai et al., 2019; Xu et al., 2020). The Cas12a-crRNA duplex was composed of 100 nM crRNA, 200 nM Cas12a, and 1 × NEBuffer 2.1. In brief, for nucleic acid detection, 5 μL of amplified product was added into 15 μL of the Cas12a-crRNA duplex to form a Cas12a-crRNA-target triplex. For real-time fluorescence monitoring, 200 nM ssDNA-FQ was added into the reaction, followed by a 45 min incubation at 37 °C in a LightCycler® 96 System (Roche, Switzerland). The fluorescence from the trans-cleavage reaction was measured every minute with excitation at 495 nm and emission at 520 nm.

For E-CRISPR analysis, the Cas12a-crRNA-target triplexes were incubated with the ssDNA modified electrode for trans-cleavage activity at 37 °C for 45 min. After treatment with the CRISPR Cas12a system, the electrode was cleaned through immersion in 10 mM Tris buffer for 5 min and then dried with nitrogen gas to prepare for electrochemical testing.

2.6. Squarewave voltammetry analysis

For SWV tests, a 10 mM Tris buffer containing 100 mM NaCl was used as the electrolyte. SWV was applied before and after the treatment of the Cas12a-crRNA-target triplex to obtain the change in current based on a potential voltage range of −0.6 to −0.1 V, a potential increment of 4 mV, a frequency of 25 Hz, and an amplitude of 25 mV. The electrochemical data was calculated as a ratio of the delta current [$\triangle I\% = (I_0 - I)/I_0$] before and after cleavage, and the significant difference in peak current is attributed to the concentration of the target bacteria.

2.7. Spiked and natural sample analysis

Artificial spiked experiment was performed according to a previous study conducted by Chen et al. (2019a). Briefly, *L. monocytogenes* ATCC 19115 was serially diluted 10-fold with normal saline solution. 1 g of each sample was added to 8 mL of the saline solution and spiked separately with 1 mL of different concentrations of diluted bacterial solution. Then, 1 mL of the matrix solution collected from each sample was subjected to DNA extraction for RAA-based E-CRISPR analysis.

For natural samples analysis, 12 *F. velutipes* plant samples were collected in Guangdong province, China. Given that the contamination level of *L. monocytogenes* in *F. velutipes* is usually low (Chen et al., 2018b), an enrichment procedure was employed prior to the RAA reaction for this experiment. Briefly, a total of 25 g of each sample was randomly selected and added to 225 mL *Listeria* enrichment broth (LB1; Guangdong Huankai Co. Ltd., Guangzhou, China) for enrichment, followed by incubation at 37 °C for 4 h. Then, 1 mL of the matrix solution collected from each sample was subjected to DNA extraction for RAA-based E-CRISPR analysis. Meanwhile, these samples were tested for the presence of *L. monocytogenes* according to the traditional culture method described in the previously reported research (Chen et al., 2019a).

3. Results and discussions

3.1. Verification of the RAA-based E-CRISPR platform for nucleic acid detection

To examine the feasibility of RAA-based E-CRISPR platform for nucleic acid detection, the *LMOSLCC2755_0090* molecular target of *L. monocytogenes* was chosen, and we obtained its partial specific dsDNA sequence by RAA amplification. The specific dsDNA sequence was identified by crRNA with a 20-nt spacer (Fig. 2A) and then the Cas12a trans-cleavage activity was activated. Owing to the preference of LbCas12a to cleave ssDNA sequences (Chen et al., 2018a), a ssDNA-FQ reporter (FAM-TTATT-BHQ1) was used in real-time fluorescence monitoring of the trans-cleavage activity of Cas12a/crRNA (Table S1). As shown in Fig. 2B, the target dsDNA sequence was successfully obtained by RAA amplification, and the sequence length was 260 bp. The fluorescence intensity of the sample with the RAA-Cas12a/crRNA complex and target DNA increased rapidly and reached saturation within 10 min. For reference, the fluorescence signal barely changed without Cas12a, crRNA, or target DNA (Fig. 2C). These results indicate that the RAA-amplified target DNA sequence can be accurately recognized by the Cas12a/crRNA complex and initiate its trans-cleavage activity to cleave the non-target ssDNA reporter.

Next, the RAA-based Cas12a was measured with the E-CRISPR platform to investigate the collateral cleavage performance on the electrode. After assembling the RAA amplified target DNA and the Cas12a/crRNA complex, the Cas12a-crRNA-target triplex complex was directly incubated on the MB-ssDNA modified electrode. Electrochemical impedance spectroscopy (EIS) was applied to characterize the interface properties of the gold electrode at different stages (Zheng et al., 2019). SWV was applied to evaluate the MB signal before and after the treatment of Cas12a-crRNA-target triplex. Fig. 2D displays the Nyquist plots of the gold electrodes at different stages and the Randles-equivalent circuit. The electron transfer resistance (R_{et}) is the main indicator and corresponds to the semicircle diameter in the Nyquist diagrams. For the bare gold electrode, the value of electron transfer resistance (R_{et}) was calculated to be 95.85 Ω using the small semicircle domain at the high frequency region. When the MB-ssDNA reporter was immobilized on the gold electrode, the value of R_{et} increased to 5875 Ω, this could be because the self-assembled negatively charged MB-ssDNA reporter monolayer caused an electrostatic repulsive force with $[Fe(CN)_6]^{3-/4-}$ (Zheng et al., 2019). After adding the Cas12a-crRNA-target triplex onto the MB-ssDNA modified electrode surface, the value of R_{et} decreased to 1693 Ω, which indicated that a large number of MB-ssDNA reporter had been trans-cleaved and separated from the electrode surface. Similarly, using the SWV detection method, the MB signal was also decreased in the presence of the cognate target with the corresponding Cas12a/crRNA (Fig. 2E). Taken together, these results demonstrate that the RAA-based E-CRISPR platform can be applied for nucleic acid detection.

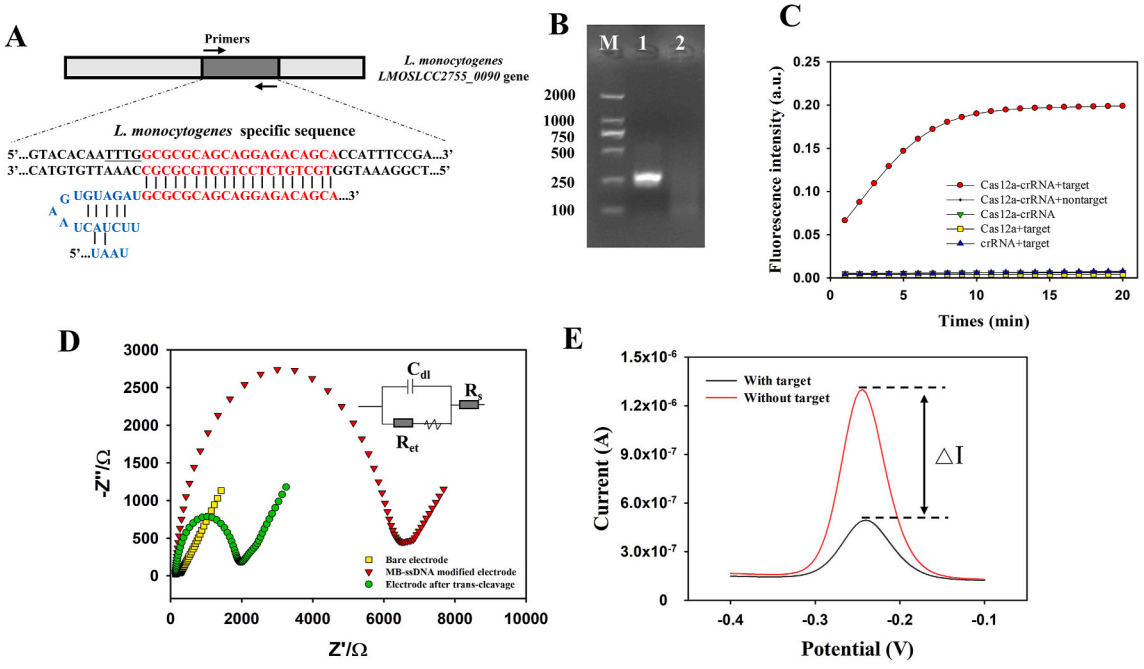


Fig. 2. Feasibility analysis of the RAA-based E-CRISPR biosensor for *L. monocytogenes* detection. (A) Design of *L. monocytogenes* cognate template and crRNA sequence. (B) Amplification of the *LMOSLCC2755_0090* gene of *L. monocytogenes* serotype by RAA. Lanes 1 and 2 correspond to RAA amplification of the gene and its negative control, respectively; Lane M is the DL2000 DNA marker. (C) Real-time fluorescence analysis of the feasibility of the RAA-based Cas12a system for non-target ssDNA cleavage. (D) Electrochemical impedance spectroscopy (EIS) characterizes the preparation and reaction process of the RAA-based E-CRISPR biosensor. EIS operating conditions were as follows: solution concentration of 10 mM $[Fe(CN)_6]^{3-/4-}$, biased potential of 0.23V (versus Ag/AgCl) in the frequency range of 0.1–10^5 Hz, and 5 mV amplitude. (E) Representation of squarewave voltammetry (SWV) evaluation of RAA-based E-CRISPR in response to *L. monocytogenes*. Red curve represents the background signal without the target, black curve represents the signal generated by the target induced trans-cleavage. (For interpretation of the references to colour in this figure legend, the reader is referred to the Web version of this article.)

3.2. Optimization of the reaction conditions

For the E-CRISPR detection platform, trans-cleavage activity is the key to signal transduction, and the concentration of Cas12a/crRNA directly influences the trans-cleavage efficiency. Therefore, multiple different concentration ratios of Cas12a/crRNA were introduced into the RAA-based Cas system and analyzed by E-CRISPR. As can be seen from Figs. S1A and 200 nM Cas12a and 100 nM crRNA exhibited the strongest current changes between the background signal and target-mediated signal. Therefore, 200 nM Cas12a and 100 nM crRNA were selected for further RAA-based E-CRISPR development. Another key factor for RAA-based E-CRISPR performance is the concentration of magnesium ions (Mg^{2+}). The divalent cation Mg^{2+} is not only essential for initiating the RAA reaction (Wang et al., 2019), but also affects the cleavage activity of Cas12a (Dai et al., 2019; Zetsche et al., 2015). The Cas12a RuvC domain cleaves ssDNA through a two-metal-ion mechanism, in which Mg^{2+} induces the conformational coordination between the RuvC domain and ssDNA by shifting the spatial distribution of ssDNA around the RuvC domains active cleavage center (Swarts et al., 2017; Yang, 2008). In this study, the RAA basic kit contained separate MgAc buffer; Mg^{2+} was also present in NEBuffer 2.1. Therefore, we evaluated different concentrations of Mg^{2+} on the trans-cleavage activity. The △I% continuously increased with increasing concentration of Mg^{2+} until it stabilized at about 20 mM. Hence, an optimized Mg^{2+} concentration of 20 mM was selected for the RAA-based Cas system (Fig. S1B). After accessing the concentrations of the complex constituents and participating ions, the optimal trans-cleavage period was also investigated. Interestingly, we found that the current continued to increase for more than 1 h (Fig. S1C). However, the cis-cleavage activity is essentially completed within 30 min according to a previous study (Chen et al., 2018a). This phenomenon shows that trans-cleavage and cis-cleavage do not occur at the same time. The cis-cleavage of the Cas12a system, initiated by target recognition, may be used as an activator of the trans-cleavage functional domain of Cas12a endonuclease (Dai et al., 2019; Xu et al., 2020). Therefore, by comprehensively evaluating the sensitivity and the detection time, a CRISPR/Cas digestion time of 45 min was used for subsequent experiments.

Next, the surface density of the ssDNA probe on the working electrode, which depends on the concentration of the MB-ssDNA reporter incubation solution, was optimized to perform efficient surface-chemistry-based trans-cleavage. As shown in Fig. S2A, the high surface density of the MB-ssDNA reporter had a lower current change value. This may be due to the steric hindrance produced by the high-density surface, thereby reducing the accessibility of Cas12a to the MB-ssDNA reporter and restricting its trans-cleavage activity. The ideal density was prepared using 1 μM of MB-ssDNA reporter and was identified as 2.5×10^{-14} mol/mm^2 (Fig. S2B), which created sufficient space for Cas12a to perform trans-cleavage on the electrode surface, providing the greatest degree of current change and ensuring the excellent detection resolution. After optimizing the electrode surface, the storage stability of the MB-ssDNA modified electrode was evaluated in a humid environment at 4 °C. The SWV signal value remained stable within one week (the signal retained > 88%), which is a sufficient turnaround time for the detection of foodborne pathogens (Fig. S3).

3.3. Sensitivity analysis of the RAA-based E-CRISPR

For the RAA-based E-CRISPR platform, both the RAA reaction and the trans-cleavage activity of Cas12a can contribute to the signal amplification. To evaluate the sensitivity of RAA-based E-CRISPR platform for *L. monocytogenes* DNA quantitation, a series of DNA concentrations of *L. monocytogenes* (ranging from 0.68×10^{-13} M to 0.68×10^{-19} M) were measured under the optimal conditions. As shown in Fig. 3A, a gradual decrease in current was observed as the DNA

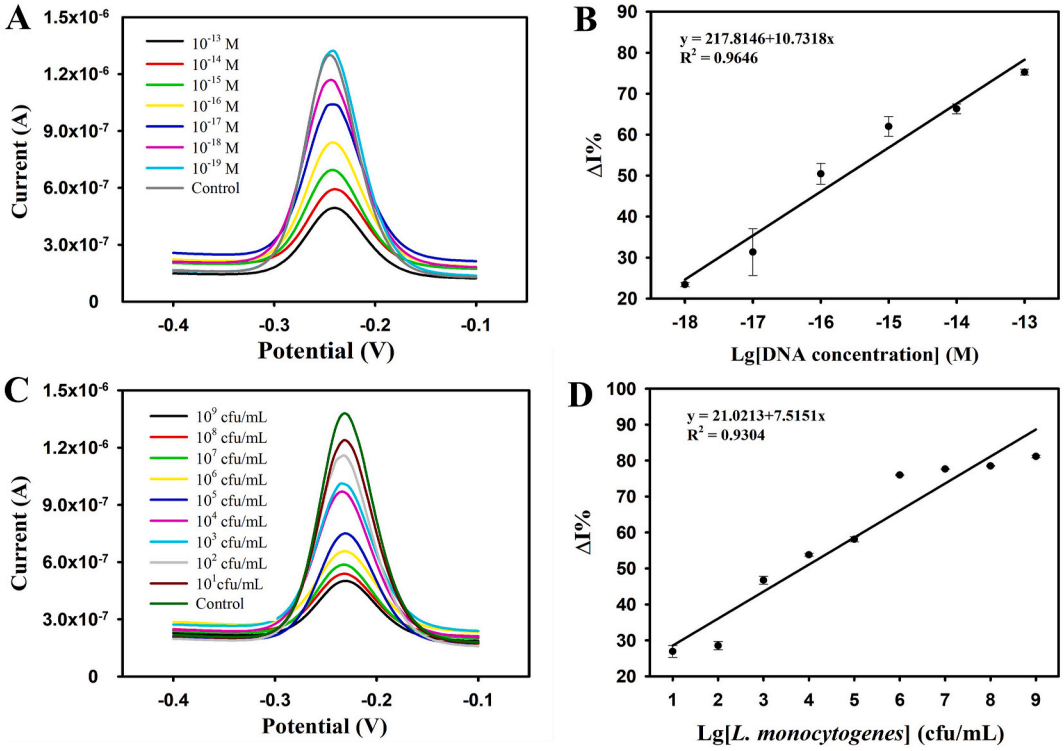


Fig. 3. Sensitivity analysis of the RAA-based E-CRISPR system. (A) The analysis results of RAA-based E-CRISPR for various concentrations of genomic DNA of *L. monocytogenes* (from 0.68×10^{-19} M to 0.68×10^{-13} M). (B) Linear relationship between the change of current and the logarithm of the amount of genomic DNA of *L. monocytogenes* (from 0.68×10^{-18} M to 0.68×10^{-13} M). (C) The analysis results of RAA-based E-CRISPR for different concentrations of *L. monocytogenes* (from 2.6×10^{1} cfu/mL to 2.6×10^{9} cfu/mL). (D) Linear relationship between the change of current and the logarithm of the concentration of *L. monocytogenes* (from 2.6×10^{1} cfu/mL to 2.6×10^{9} cfu/mL). Control refers to replacing the template with H_2O. Error bars represent mean ± SD, where n = 3 replicates.

concentrations of *L. monocytogenes* increased. The change of current was linearly related to the logarithms of *L. monocytogenes* DNA concentration, this was mapped with the correlation equation $\triangle I\% = 217.8146 + 10.7318\ lgC_{L.\ monocytogenes\ DNA}$, furthermore the R^2 was calculated to be 0.9646 (Fig. 3B). A background (B) experiment was conducted without using the target DNA, in which the mean current change value of the background (n = 3) plus three standard deviations (SD), B+3SD was calculated and used as a cut-off value for determination of positivity and negativity (Kim et al., 2016; Low et al., 2013). In this study, the calculated cut-off value was 14.77%. Experiments with current change values ≥ 14.77% were interpreted as positive, while those below were defined as negative. Based on the cut-off value, the calculated limit of detection can reach 0.68 aM (0.68×10^{-18} M). Compared to a previous study about Cas12a mediated E-CRISPR detection of nucleic acids [limit-of-detection (LOD) was 5×10^{-11} M] (Dai et al., 2019), the calculated LOD of our RAA-based E-CRISPR was approximately 10^8-fold lower, which is also superior to most previously reported E-CRISPR based diagnostics in terms of sensitivity (Table S3) (Bruch et al., 2019; Dai et al., 2019; Hajian et al., 2019; Xu et al., 2020; Zhou et al., 2020). Furthermore, the LODs of the RAA-based E-CRISPR and the RAA-based Cas12a fluorescence detection were also compared. A ssDNA-FQ probe was used as reporter of RAA-based Cas12a fluorescence detection. The experimental results are shown in Fig. S4; the LOD of RAA-based Cas12a was calculated to be 0.68×10^{-17} M. Thus, E-CRISPR can potentially improve the sensitivity by 10-fold. This sensitivity of RAA-based E-CRISPR assay is also superior to previously reported CRISPR/Cas based fluorescence detection methods (He et al., 2020; Wang et al., 2019) and other sensing methods, such as surface-enhanced Raman scattering (Kim et al., 2020) and lateral flow assay (Mukama et al., 2020).

Next, we further validated the RAA-based E-CRISPR detection of different concentrations of *L. monocytogenes* in pure cultures (2.6×10^9–2.6×10^1 cfu/mL). As shown in Fig. 3C and D, a gradual decrease in current was observed as the concentration of *L. monocytogenes* increased. The change of current was linearly related to the logarithms of the concentration of *L. monocytogenes* with a correlation equation of $\triangle I\% = 21.0213 + 7.5151\ lgC_{L.\ monocytogenes}$ ($R^2 = 0.9304$). The calculated detection limit of this assay was 26 cfu/mL.

3.4. Specificity analysis of the RAA-based E-CRISPR

In addition to the flexible programmability of crRNA and the effective signal amplification efficiency of Cas12a, the high selectivity of the Cas12a/crRNA system is another important advantage. It has been previously confirmed that the Cas12a/crRNA-based direct nucleic acid detection systems have single-base resolution (Chen et al., 2018a; Gootenberg et al., 2018). In addition, the introduction of the RAA method can not only improve the sensitivity, but also help to ensure the specificity through the precise identification of the target DNA sequence. In this study, the specificity of RAA-based E-CRISPR platform was investigated with 15 bacterial strains (Table S2). The target DNA extracted from 10^7 cfu/mL of the *L. monocytogenes* strains exhibited significant signal changes ($\triangle I\% > 70\%$), whereas the signal changes were low in the detection of non-*L. monocytogenes* strains (10^8 cfu/mL), which were comparable to the signal changes obtained from the blank control, thereby indicating the superior selectivity of the RAA-based E-CRISPR in differentiating *L. monocytogenes* from non-target species (Fig. 4).

3.5. Analyzing the performance of RAA-based E-CRISPR for the detection of L. moncytogenes in spiked and natural F. velutipes samples

To verify the feasibility of the RAA-based E-CRISPR method to detect *L. monocytogenes* in food matrices, *F. velutipes* samples were spiked with serially diluted *L. monocytogenes* (from 9.4×10^7 cfu/mL to 9.4×10^0 cfu/mL), the DNA was then extracted for detection. As shown in Fig. 5A,

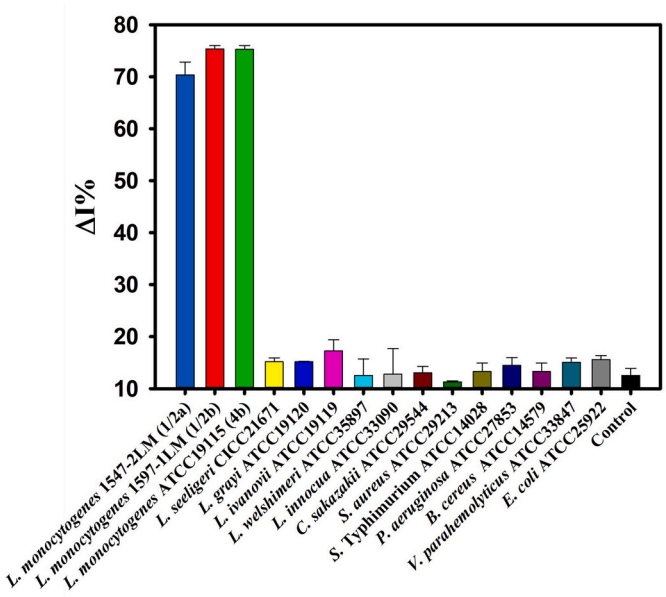


Fig. 4. Specificity analysis of the RAA-based E-CRISPR system. The change in signal was calculated based on the SWV current with the addition of the target *L. monocytogenes* (10^7 cfu/mL) and non-target bacteria (10^8 cfu/mL), respectively. Control refers to replacing the template with H_2O. Error bars represent mean ± SD, where n = 3 replicates.

a gradual decrease in current was observed as the concentrations of *L. monocytogenes* increased. Considering that the 10 mL matrix solution corresponds to 1 g of sample, a unit conversion was performed according to the sample quality. The change of current was linearly related to the logarithms of the *L. monocytogenes* concentration in the spiked sample; the correlation equation was $\triangle I\% = 11.7817 + 8.5309\ lgC_{L.\ monocytogenes}$, and the R^2 was calculated to be 0.9183 (Fig. 5B). The calculated LOD of the RAA-based E-CRISPR method in spiked samples was 9.4×10^2 cfu/g. According the EU food safety regulations limit *L. monocytogenes* to <100 cfu/g at the end of the shelf-life of a food product (Ziegler et al., 2019). Therefore, it is necessary to perform pre-enrichment treatment or combine with magnetic separation method before the RAA reaction in this experiment to achieve the detection of low-contamination samples.

Moreover, the application ability of RAA-based E-CRISPR was evaluated for the detection of *L. monocytogenes* in 12 natural *F. velutipes* samples (Table S4). The National Food Safety Standard of China (GB4789.30–2016) was performed to validate the accuracy of the RAA-based E-CRISPR. Genomic DNA was extracted from the natural samples and added to the reaction system (Fig. 6A). As shown in Fig. 6B and C, and Table S4, a cut-off value (B+3SD) of 19.94% was calculated from the background (B) experiment which was conducted in triplicate using *F. velutipes* samples without *L. monocytogenes*. Based on the cut-off value, only two samples were positive, and the RAA-based E-CRISPR method corroborated 100% with the conventional culture. The assay showed a fast response and required no expensive materials such as fluorescent instruments or monoclonal antibodies. Furthermore, apart from the fluorescence reporter, the usage of E-CRISPR enabled us to improve the sensitivity. Therefore, our method holds a promising potential for the rapid detection of pathogenic bacteria in clinical or food samples.

4. Conclusion

In this study, we developed a RAA-based E-CRISPR biosensor for ultrasensitive and highly specific detection of *L. monocytogenes*. Compared to previous Cas12a based signal amplification strategies, the RAA-based E-CRISPR platform not only takes full advantage of the specific RNA recognition ability of Cas12a to achieve high specificity,

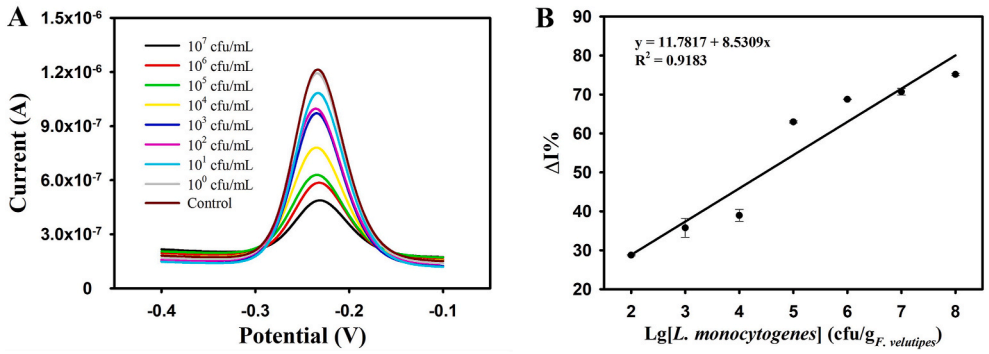


Fig. 5. Analyzing the performance of the RAA-based E-CRISPR platform for the detection of *L. monocytogenes* in spiked samples. (A) Analysis of the test results of RAA-based E-CRISPR for different concentration of *L. monocytogenes* in spiked *F. velutipes* samples (from 9.4 × 10^0 cfu/mL to 9.4 × 10^7 cfu/mL). (B) Linear relationship between the change of current and the logarithm of the concentration of *L. monocytogenes* in spiked *F. velutipes* samples (from 9.4 × 10^2 cfu/g to 9.4 × 10^8 cfu/g). Control refers the background experiment without *L. monocytogenes*. Error bars represent mean ± SD, where n = 3 replicates.

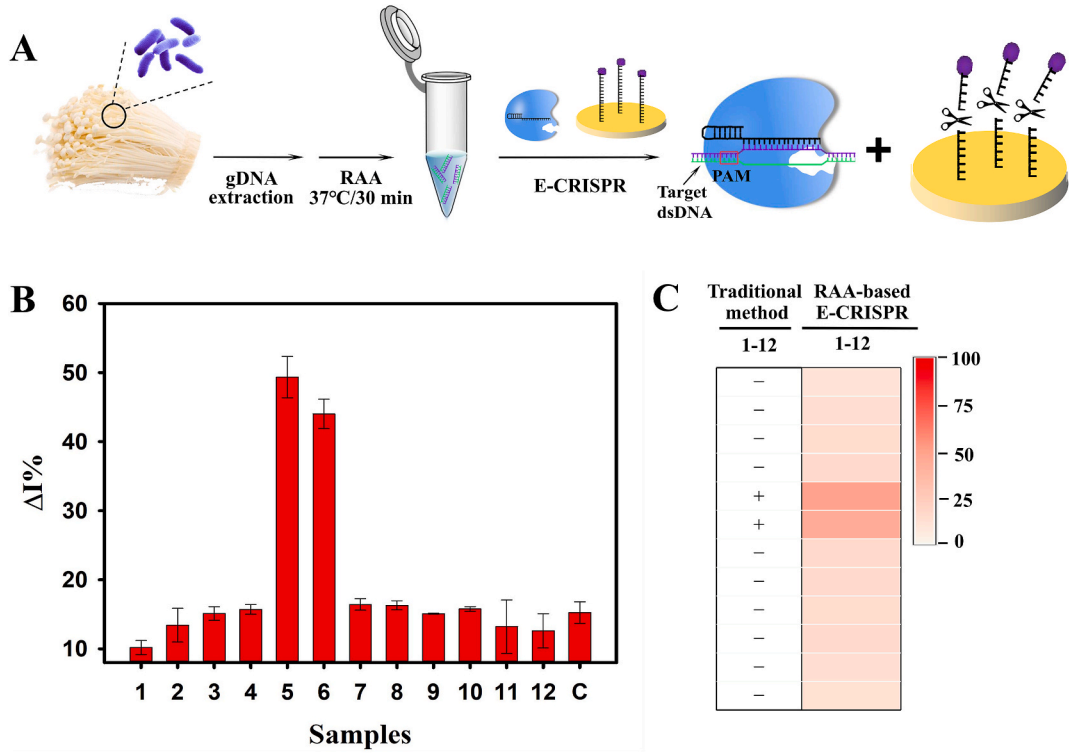


Fig. 6. The applicability of the RAA-based E-CRISPR platform to detect *L. monocytogenes* in natural samples. (A) Schematic outlining DNA extraction from *F. velutipes* samples for *L. monocytogenes* detection by the RAA-based E-CRISPR biosensor. (B) The change of signal was calculated based on the SWV current with the addition of genomic DNA extracted from different samples. (C) Detection of L. *monocytogenes* in 12 *F. velutipes* samples by conventional culture method (left) and RAA-based E-CRISPR biosensor (right). Control refers the background experiment without *L. monocytogenes*. The RAA-based E-CRISPR biosensor heatmap represents normalized mean current signal change values. Error bars represent mean ± SD, where n = 3 replicates.

but also converts the target recognition activity into a detectable electrochemical signal to improve the sensitivity. In optimized conditions, the platform can provide the calculated detection limits of 0.68 aM genomic DNA and 940 cfu/g for *L. monocytogenes* in spiked sample, respectively. More importantly, the E-CRISPR biosensor as a reliable method can be applied not only to the Cas12a system to accurately identify *L. monocytogenes*, but also to other Cas systems by rationally designing crRNA to achieve either pathogenic bacteria or nucleic acid detection. Therefore, the RAA-based E-CRISPR method can be utilized in many nucleic acid biosensing platforms, thus promoting the development of biosensors and improving food safety monitoring and robust point-of-care diagnostic systems.

CRediT authorship contribution statement

Fan Li: Investigation, Methodology, Data curation, Writing - original draft. **Qinghua Ye:** Project administration, Data curation. **Moutong Chen:** Project administration, Data curation. **Baoqing Zhou:** Data curation. **Jumei Zhang:** Supervision, Resources. **Rui Pang:** Data curation. **Liang Xue:** Validation. **Juan Wang:** Validation. **Haiyan Zeng:** Validation. **Shi Wu:** Validation. **Youxiong Zhang:** Data curation. **Yu Ding:** Supervision, Conceptualization. **Qingping Wu:** Supervision, Writing - review & editing.

Declaration of competing interest

The authors declare that they have no known competing financial interests or personal relationships that could have appeared to influence the work reported in this paper.

Acknowledgements

The authors would like to thank to the College of Food Science and Technology of Nanjing Agricultural University and the State Key Laboratory of Food Science and Technology of Nanchang University for donating strains. The work was funded by the National Key Research and Development Program of China (2018YFC1604201), National Natural Science Foundation of China (31901783), Key Research and Development Program of Guangdong Province, China (2019B020209001), GDAS′ Project of Science and Technology Development (2019GDASYL-0201001, 2018GDASCX-0102).

Appendix A. Supplementary data

Supplementary data to this article can be found online at https://doi.org/10.1016/j.bios.2021.113073.

References

Arroyo-Curras, N., Dauphin-Ducharme, P., Ortega, G., Ploense, K.L., Kippin, T.E., Plaxco, K.W., 2018. ACS Sens. 3, 360–366.
Bruch, R., Baaske, J., Chatelle, C., Meirich, M., Urban, G.A., 2019. Adv. Mater. 31, 1905311.
Chen, J.S., Ma, E., Harrington, L.B., Da Costa, M., Tian, X., Palefsky, J.M., Doudna, J.A., 2018a. Science 360, 436–439.
Chen, M., Cheng, J., Pang, R., Zhang, J., Chen, Y., Zeng, H., Lei, T., Ye, Q., Wu, S., Zhang, S., Wu, H., Wang, J., Wu, Q., 2019a. LWT - Food Sci. Technol. (Lebensmittel-Wissenschaft -Technol.) 116, 108474.
Chen, M., Cheng, J., Wu, Q., Zhang, J., Chen, Y., Zeng, H., Ye, Q., Wu, S., Cai, S., Wang, J., Ding, Y., 2018b. Front. Microbiol. 9, 1711.
Chen, M., Cheng, J., Zhang, J., Chen, Y., Zeng, H., Xue, L., Lei, T., Pang, R., Wu, S., Wu, H., Zhang, S., Wei, X., Zhang, Y., Ding, Y., Wu, Q., 2019b. Front. Microbiol. 10, 946.
Chen, M., Wu, Q., Zhang, J., Guo, W., Yang, X., 2014. Foodb. Pathog. Dis. 11, 620–627.
Dai, Y., Liu, C.C., 2019. Angew. Chem. Int. Ed. 131, 12483–12496.
Dai, Y., Somoza, R.A., Wang, L., Welter, J.F., Li, Y., Caplan, A.I., Liu, C.C., 2019. Angew. Chem. Int. Ed. 58, 17399–17405.
Dai, Y., Wu, Y., Liu, G., Gooding, J.J., 2020. Angew. Chem. Int. Ed. 132, 20938–20950.
Dauphin-Ducharme, P., Arroyo-Curras, N., Plaxco, K.W., 2019. J. Am. Chem. Soc. 141, 1304–1311.
Gootenberg, J.S., Abudayyeh, O.O., Kellner, M.J., Joung, J., Collins, J.J., Zhang, F., 2018. Science 360, 439–444.
Gootenberg, J.S., Abudayyeh, O.O., Lee, J.W., Essletzbichler, P., Dy, A.J., Joung, J., Verdine, V., Donghia, N., Daringer, N.M., Freije, C.A., 2017. Science 356, 438–442.
Hajian, R., Balderston, S., Tran, T., Deboer, T., Etienne, J., Sandhu, M., Wauford, N.A., Chung, J.Y., Nokes, J., Athaiya, M., 2019. Nat. Biomed. Eng. 3, 427–437.
He, Q., Yu, D., Bao, M., Korensky, G., Chen, J., Shin, M., Kim, J., Park, M., Qin, P., Du, K., 2020. Biosens. Bioelectron. 154, 112068.
Horvath, P., Barrangou, R., 2010. Science 327, 167–170.
Huang, Z., Tian, D., Liu, Y., Lin, Z., Lyon, C., Lai, W., Fusco, D., Drouin, A., Yin, X., Hu, T., Ning, B., 2020. Biosens. Bioelectron. 164, 112316.
Kim, D., Garner, O.B., Ozcan, A., Di Carlo, D., 2016. ACS Nano 10, 7467–7475.
Kim, H., Lee, S., Seo, H.W., Kang, B., Moon, J., Lee, K.G., Yong, D., Kang, H., Jung, J., Lim, E.-K., 2020. ACS Nano 14, 17241–17253.
Kim, J., Campbell, A.S., Ávila, E.F.D., Wang, J., 2019. Nat. Biotechnol. 37, 389–406.
Konermann, S., Brigham, M.D., Trevino, A.E., Joung, J., Abudayyeh, O.O., Barcena, C., Hsu, P.D., Habib, N., Gootenberg, J.S., Nishimasu, H., 2015. Nature 517, 583–588.
Li, F., Ye, Q., Chen, M., Zhang, J., Xue, L., Wang, J., Wu, S., Zeng, H., Gu, Q., Zhang, Y., Wei, X., Ding, Y., Wu, Q., 2021. Front. Microbiol. 11, 634255.
Lomonaco, S., Decastelli, L., Nucera, D., Gallina, S., Bianchi, D.M., Civera, T., 2009. Int. J. Food Microbiol. 128, 516–520.
Low, K.-F., Karimah, A., Yean, C.Y., 2013. Biosens. Bioelectron. 47, 38–44.
McLauchlin, J., 1990. Epidemiol. Infect. 104, 191–201.
Mukama, O., Yuan, T., He, Z., Li, Z., de Dieu Habimana, J., Hussain, M., Li, W., Yi, Z., Liang, Q., Zeng, L., 2020. Sensor. Actuator. B Chem. 316, 128119.
Myhrvold, C., Freije, C.A., Gootenberg, J.S., Abudayyeh, O.O., Metsky, H.C., Durbin, A. F., Kellner, M.J., Tan, A.L., Paul, L.M., Parham, L.A., 2018. Science 360, 444–448.
Swarts, D.C., van der Oost, J., Jinek, M., 2017. Mol. Cell 66, 221–233.
Tang, Y., Fu, Y., 2018. Cell Biosci. 8, 1–13.
Van Dongen, J.E., Berendsen, J.T., Steenbergen, R.D., Wolthuis, R.M., Eijkel, J.C., Segerink, L.I., 2020. Biosens. Bioelectron. 166, 112445.
Wang, B., Wang, R., Wang, D., Wu, J., Li, J., Wang, J., Liu, H., Wang, Y., 2019. Anal. Chem. 91, 12156–12161.
Wang, M., Zhang, R., Li, J., 2020. Biosens. Bioelectron. 166, 112430.
Xu, W., Jin, T., Dai, Y., Liu, C.C., 2020. Biosens. Bioelectron. 155, 112100.
Yang, W., 2008. Nat. Struct. Mol. Biol. 15, 1228–1231.
Zetsche, B., Gootenberg, J.S., Abudayyeh, O.O., Slaymaker, I.M., Makarova, K.S., Essletzbichler, P., Volz, S.E., Joung, J., Van Der Oost, J., Regev, A., 2015. Cell 163, 759–771.
Ziegler, M., Kent, D., Stephan, R., Guldimann, C., 2019. Int. J. Food Microbiol. 296, 83–92.
Zheng, Y., Xu, Y., Lin, L., Li, Y., Chen, W., Chen, J., Lei, Y., Lin, L., Liu, A., Lin, X., 2019. J. Electroanal. Chem. 840, 165–173.
Zhou, T., Huang, R., Huang, M., Shen, J., Xing, D., 2020. Adv. Sci., 1903661